The Cryosphere Discuss., 5, 2319–2347, 2011
www.the-cryosphere-discuss.net/5/2319/2011/
doi:10.5194/tcd-5-2319-2011

The Cryosphere Discussions

Surface mass budget and meltwater discharge from the Kangerlussuaq sector of the Greenland ice sheet during record-warm year 2010

D. van As[1], A. Hubbard[2], B. Hasholt[3], A. B. Mikkelsen[3], M. van den Broeke[4], and R. S. Fausto[1]

[1]Geol. Survey of Denmark and Greenland, Øster Voldgade 10, 1350 Copenhagen K, Denmark
[2]Institute of Geography and Earth Sciences, Aberystwyth University, Llandinam Building, Penglais Campus, Aberystwyth, SY23 3DB, Wales
[3]Department of Geography and Geology, Øster Voldgade 10, 1350 Copenhagen K, Denmark
[4]Institute for Marine and Atmospheric Research, Utrecht University, Princetonplein 5, 3584 CC Utrecht, The Netherlands

Received: 15 August 2011 – Accepted: 28 August 2011 – Published: 6 September 2011

Correspondence to: D. van As (dva@geus.dk)

Published by Copernicus Publications on behalf of the European Geosciences Union.

Abstract

The year 2010 has been anomalously warm in most of Greenland, most notably in the south and along the western coast. Our study targets the Kangerlussuaq region around 67° N in Southwest Greenland, where the temperature anomalies were record setting. In 2010, the average temperature was 5° C (2.7 standard deviations) above the 1974–2010 average in the town of Kangerlussuaq. High temperatures were also observed over the ice sheet, with the positive anomaly increasing with altitude. Also surface albedo, from calibrated MODIS measurements, was anomalously low in 2010, chiefly in the upper ablation zone. The low albedo was caused by the high ablation in 2010, which profited in turn from high temperatures, low albedo, and of low wintertime accumulation. The largest melt excess (166 %) was found in the upper ablation zone, where higher temperatures and lower albedo contributed equally to the melt anomaly. In total, we estimate that 6.6 km^3 of surface meltwater ran off the ice sheet in the Kangerlussuaq catchment area in 2010, exceeding "normal" year 2009 by 145 %. When compared to discharge estimated from discharge measurements in the proglacial river we find good agreement. The time lag between the records is caused by storage within and underneath the ice sheet, and suggests adaption of the subglacial drainage system to meltwater availability, with more efficient drainage occurring after the peak of the melt season.

1 Introduction

Greenland stores nearly 3 million km^3 of ice, a large potential contribution to sea level rise. In recent years increasingly large sections of the Greenland ice sheet have been losing mass, as determined from its satellite-derived gravity field (Khan et al., 2010; Schrama et al., 2011). Whereas the retreat and thinning of numerous floating outlet glaciers has not been limited to recent years (Csatho et al., 2008), the acceleration of many major ice streams and a consequential increase in iceberg discharge is a current development (Rignot and Kanagaratnam, 2006; Howat et al., 2011). However, mass loss is not confined to regions with marine-terminating glaciers. Large sections of the land-terminating ice sheet margin are known to be subject to thinning (Pritchard et al., 2009) as a direct and indirect consequence of increased surface melt. Roughly half of recent Greenland ice sheet mass loss can be attributed to increases in surface melt (van den Broeke et al., 2009), which reaffirms the importance of monitoring the surface mass budget of the ice sheet.

Temperatures in Greenland have been monitored since the 1870s. After a 40 yr cooling period a warming trend has set in since the 1980s (Box, 2002). The 1990s experienced the strongest warming on record, and the 2000s have had several record-setting years in various Greenland regions, though mostly on the west coast. But 2010 was the warmest year in most of Greenland (except the northeast) since the start of meteorological observations (personal communication J. Cappelen; Box et al., 2011). The effects of high temperatures and low precipitation on 2010 ablation, and/or the albedo feedback functioning as an amplifier, has been discussed by Tedesco et al. (2011), van den Broeke et al. (2011) and van As et al. (2011).

In light of the extraordinary atmospheric conditions in Greenland in 2010, in this paper we investigate surface melt near Kangerlussuaq, Southwest Greenland, using data of a relatively dense network of automatic weather stations (AWS) that is operational in the area. First we quantify the 2010 temperature and MODIS-derived albedo anomalies for the Kangerlussuaq region, then we calculate surface ablation and meltwater run-off, validate results using ablation and meltwater discharge measurements, and investigate the causes for the 2010 melt anomaly.

TCD
5, 2319–2347, 2011

2 Methods

2.1 Observations

Monitoring the surface mass and energy budget of the ice sheet is done best by making use of on-ice AWS. The Kangerlussuaq region of the Greenland ice sheet has the highest density of AWS on the otherwise scarcely instrumented ice sheet (Fig. 1), and therefore is the most suitable location to investigate factors influencing surface melt. Here, the Institute for Marine and Atmospheric Research in Utrecht (IMAU) has been running 3 AWS since 2003 (S5, S6 and S9). In 2008 and 2009 the Geological Survey of Denmark and Greenland (GEUS) added 3 stations to the transect (KAN_L, KAN_M and KAN_U) as part of the Greenland Analogue Project (GAP). See Table 1 for station metadata. The equilibrium line in this region is situated at a relatively high altitude ($\sim$1500 m), meaning that 5 AWS are located in the ablation zone. KAN_U is placed well into the accumulation zone, though melt does occur there at the peak of the melt season. We tested the possibility of extending our region of interest to the ice divide by including the Greenland Climate Network (GC-Net) stations DYE-2 and Saddle (resp. 66 and 158 km southeast of KAN_U), but found a too low correlation between those stations and the ones included in the study; including these in the study may complicate the interpretation of results while surface melt and run-off values will not be impacted much.

For melt calculation we make use of the following weather-station observations at 2–3 m above the surface: air pressure, air temperature, relative humidity, wind speed, and incoming shortwave/solar and longwave/terrestrial radiation. Reflected shortwave radiation, emitted longwave radiation, and surface height change due to accumulation and ablation are also used, but for calibration and validation purposes (see below).

For model input data we interpolate daily-mean AWS observations to 100 m elevation bins to be able to determine the distributed melt patterns in the region. Although the Kangerlussuaq sector of the ice sheet has a relatively high density of AWS, distances between stations are still up to 54 km (Fig. 1), and interpolation of all measured variables required for surface mass budget modelling is not guaranteed to give satisfactory accuracy in melt calculation. Multiple interpolation methods were tested, and we chose to apply a linear least-squares fit to all stations for every time step, since this fit allows a fairly reliable extrapolation outside the vertical domain with weather station observations, and is deemed applicable for melt modelling.

Surface albedo is one of the most important input variables, but cannot be interpolated from AWS observations due to its large spatial variability. Therefore we use satellite-derived albedo from the Moderate Resolution Imaging Spectroradiometer (MODIS) on NASA's Terra satellite, after applying corrections to remove sensitivity to the solar zenith angle as identified by comparing the MODIS data to the observed albedo at the AWS. Issues with the MODIS albedo product over Greenland snow surfaces for large zenith angles were identified by Wang and Zender (2010), which was however commented on by Schaaf et al. (2011). We consider our approach a step towards MODIS validation over Greenland bare ice surfaces, but mostly a large improvement in regional melt modelling, since previous studies assumed ice albedo to be spatially and temporally constant.

River depth and flow velocity data gathered at the bridge in the town of Kangerlussuaq were converted into freshwater flux with an estimated uncertainty of 20 % for single values (Hasholt et al., 2011). Just past the bridge, the freshwater from the 25 km long proglacial river originating at the ice sheet margin enters Kangerlussuaq fjord. Upstream of the bridge two proglacial rivers merge, of which the northernmost one originates from the snouts of two unnamed glaciers that are often referred to as "Russell Glacier" and "Leverett Glacier".

In the melt model calculations, the catchment areas of both rivers were taken into account to be able to compare calculated surface meltwater run-off to observed river discharge at the bridge. From hereon we call the combined areas the "Kangerlussuaq catchment area". Since automated tools such as provided with ArcGIS have proven inaccurate over smooth, sloping surfaces with low aspect ratios, we determined the drainage basin boundaries by hand from our digital elevation model of the ice sheet.

Ideally, we would use the catchment as delineated from the subglacial topography, since meltwater in the Kangerlussuaq catchment area does not run over the ice sheet surface long before a moulin transports it to en- or subglacial conduits. Since no accurate map of subglacial topography exists at this point, we had to use surface topography to delineate the Kangerlussuaq catchment. This will be further discussed in the results section.

2.2 Surface mass budget model

Near-surface air temperature impacts melt through the turbulent flux of sensible heat and incoming longwave radiation, so it is only one of the contributors to surface melt of glaciers and ice caps. To accurately determine to what extent the atmospheric conditions in 2010 impacted the nearby ice sheet in the Kangerlussuaq region, we must apply a surface energy balance model. The model used here is similar to that applied by van As (2011). It uses multiple meteorological observations (air pressure, temperature, humidity, wind speed, and the down-welling components of shortwave radiation and longwave radiation) to calculate the surface energy budget components (absorbed shortwave radiation, net longwave radiation, sensible heat flux, latent heat flux, subsurface heat flux, rain heat flux). If the energy budget components are not in balance, the surplus energy is used to melt snow or ice. The surface mass budget is the sum of solid precipitation, melt, and sublimation/deposition. Precipitation is parameterized and tuned to accumulation observations; we prescribe a 1 mm water equivalent per hour precipitation rate for periods with a heavy cloud cover, when incoming longwave radiation values exceed blackbody radiation calculated using near-surface air temperature. Meltwater produced at the surface refreezes in underlying snow layers if temperature and density requirements are met, i.e. when sub-surface grid cells are at sub-freezing temperatures and not at ice density.

Discussion Paper | Discussion Paper | Discussion Paper | Discussion Paper |

TCD

5, 2319–2347, 2011

Greenland surface mass budget and melt in 2010

D. van As et al.

2.3 Model uncertainty and validation

Several factors contribute to the uncertainty in our surface energy budget calculations. Firstly, measurement errors vary per sensor and add up in the nonlinear surface energy budget calculations. The largest sensor uncertainty as reported by the manufacturer is for the Kipp & Zonen CNR1 radiometer (10 % for daily totals, see van As, 2011), which is actually reported to be smaller (van den Broeke et al., 2004). Secondly, a number of assumptions are made in our model, most importantly for the aerodynamic surface roughness length (chosen to be 1×10^{-3} m for momentum for ice, and 1×10^{-4} m for snow, which are common values as listed by Brock et al., 2006). Assuming these to be constant in time is a simplification, as outlined by Smeets and van den Broeke (2008). The linear interpolation of measured variables further contributes to model uncertainty; alternatively, it keeps measurement errors by single AWS in check by the measurements of other stations. Finally, in calculating the integrated run-off from the ice sheet, the error in the delineation of the Kangerlussuaq catchment area translates directly into run-off errors. All in all, as a conservative educated guess we will use a 15 % uncertainty for daily melt totals.

Evaluation of the calculations is performed using three independent methods. Firstly, we require a close agreement between the modelled surface temperatures and those calculated from measured emitted longwave radiation assuming black-body radiative properties. We found RMSD values of 1.0–1.7 °C for the six stations and their corresponding elevation bins, which is 4–6 times smaller than the uncertainty derived from the 10 % uncertainty statement by the radiometer manufacturer. This testifies for accurately modelled surface temperatures, as well as for more accurate radiometer readings than specified by the manufacturer. Secondly, below we compare observed and modelled surface height change due to ablation and accumulation at the AWS sites. Thirdly, we assess the quantitative agreement between the surface meltwater run-off for the Kangerlussuaq catchment area and the freshwater discharge estimates at the Kangerlussuaq bridge.

3 Results

3.1 Temperature

The earliest continuous meteorological records by the Danish Meteorological Institute (DMI) in the town of Kangerlussuaq date back to May 1973. Over the 38+ yr period since then, the mean temperature trend showed warming by 0.067 °C per year, which is partly due to cold years in the early 1980s and partly due to persistent high mean temperatures since 1996. Figure 2 confirms that the year 2010 ranks warmest in Kangerlussuaq, as it does in other Greenlandic regions. Whereas the 1974–2010 temperature record gives a mean value of −5.0 °C, the 2010 average was −0.1 °C, 2.7 standard deviations above average. This well exceeded both the second (2005) and third (2003) warmest years by 2.5 °C.

Unique for 2010 was also that all months experienced above-average temperatures. January, February, November and December exceeded the monthly average by 7–11 °C, showing that winter temperatures contributed much to the high yearly average temperature. The months May, August, and December were the warmest of these particular months in the entire 37 yr period. Similarly, April, September, and November 2010 were among the warmest 3 of these months in the whole time series.

As mentioned, these high temperatures occurred in all of Greenland, the northeast excluded. A large-scale perspective is provided by Box et al. (2011), who reported that yearly temperatures in several West and South Greenland towns all were 3 standard deviations above the 1971–2000 baseline. Van As et al. (2011) showed that temperatures in South Greenland were 2.0 °C (4.7 standard deviations) above the 2000–2009 decade average, which is the warmest decade on record. They mentioned the warmest months to be November, May, August, December and September (in order of excess).

The extraordinary temperatures in Kangerlussuaq in 2010 are contrasted by those in 2009, which with a yearly-mean temperature of −4.7 °C were close to average: 0.3 °C above the 1974–2010 norm. During the months April to August the temperatures departed only 0–0.8 °C from their long-term averages, whereas September and October were about 1 °C colder than average. Thus in terms of summer temperatures and length of the melt season, 2009 qualifies as a year that is typical for the 1974–2010 period. From hereon, we will use the conditions in 2009 as a reference for the anomalous year of 2010.

In Fig. 3 the 2009 and 2010 near-surface temperatures over the ice sheet are compared at four different elevations above sea level (500 m: lower ablation zone, 1000 m: middle ablation zone, 1500 m: equilibrium line altitude, and 2000 m: lower accumulation zone). The plots show the results of the linear interpolation to the 6 weather stations in the Kangerlussuaq catchment area. Remarkably, 2010 temperatures exceed those in the previous year throughout the year (note that these are 30 day running means) and at all elevations, given the positive values of the thick lines showing the 2010–2009 difference. During periods outside the high melt season (September to May) annual variability can be large, as also seen in Fig. 2. For instance, 2010 temperatures in warm months May and September exceed those of 2009 by more than 5 °C. Differences during the high-melt months of June, July and August are commonly smaller, as seen from the smaller 2010 excess values in Fig. 3, because near-surface temperatures are moderated by the proximity of the melting ice sheet surface.

Exceptional is the month of August 2010, when chiefly in the higher regions of the transect anomalously high temperatures prevailed. In the lower accumulation zone temperatures exceeded 2009 temperatures by as much as 5 °C. Thus the heat in the extreme month of August 2010 in Kangerlussuaq was reflected in high near-surface temperatures at high elevation over the ice sheet, but not closer to the ice sheet margin. However, as downwelling longwave radiation measurements will show below, free-atmospheric temperatures were high along the entire transect. This indicates that in regions where melt is common, an increase in free-atmospheric temperature only has a limited effect on near-surface temperature due to the moderating presence of the melting ice surface. Higher up the glacier, where cold spells of sub-freezing temperatures occur throughout the melt season, the response to warm weather will be larger.

TCD
5, 2319–2347, 2011

3.2 Surface albedo

Surface albedo for the Kangerlussuaq section of the Greenland ice sheet is investigated using MODIS satellite imagery up to and including 2010. As is common, albedo on average increases with surface elevation, and drops during the melt season (Fig. 4). At 2000 m, albedo values throughout the year are typical for fresh snow surfaces (0.8–0.9). Ice values (below about 0.6) are not measured near the equilibrium line altitude of 1500 m, but are typical in the middle ablation zone at 1000 m elevation in the months July and August. In the lower ablation zone (500 m) albedo drops below 0.6 for four months, and does not reach high "snow" values often since winter accumulation totals are small here (van den Broeke et al., 2008).

In 2010, albedo was lower than the decade average at all elevations during the entire melt season (lower panel in Fig. 4). In the lower and middle ablation zone (500 and 1000 m) albedo dropped 0.1 below the average already in May, since melt had occurred a few weeks earlier than in other years. At 1000 m this effect was most prominent, where ice was exposed even before June (albedo below 0.6). Whereas in the lower ablation zone albedo returned to near-normal values in July 2010, since high melt occurs here every year, in the higher regions of the ablation zone it remained at least 0.1 below average until mid-September, causing much higher solar absorption rates than usual (up to 40 %). In the upper ablation zone the lowest 2010 albedo anomalies were attained in August, coincident with the high-elevation warm episode discussed in the previous section. Temperature and albedo anomalies are likely to have enhanced each other (melt-albedo feedback), in which high temperatures cause high melt, lowering albedo due to enhanced surface metamorphosis, increasing solar radiation absorption, and thus melt.

Note that the MODIS albedo in Fig. 4 has been calibrated using the albedo determined at KAN_L, M and U, using a solar-elevation correction function. A consequence of this is that the drop in albedos after the equinox (21 June) may be exaggerated, as is for instance seen at 2000 m. Whereas the albedo calibration may not be suitable for

TCD
5, 2319–2347, 2011

a detailed albedo study, we will show below that this calibration improves the accuracy of our melt model considerably and is therefore suitable for the purpose of this study.

3.3 Wintertime accumulation

Besides high temperatures and low surface albedo, a third cause for extreme ablation in 2010 in Southwest Greenland could have been low wintertime accumulation: the more snow has accumulated, the longer it takes for the bare ice to surface during the melt season. Tedesco et al. (2011) reported that indeed this was one of the causes for high ablation in 2010. We do not investigate the effect of low accumulation in this paper, nor is it of large consequence to our meltwater run-off calculations since the lower regions of the Kangerlussuaq catchment area receives little precipitation due to orographic shielding towards the southwest and probably significant wintertime snow-drift sublimation (van den Broeke et al., 2008). Up to 1000 m elevation, less than a few decimetres of snow accumulate on the ice sheet each winter, not taking into account snow that settles in crevasses. This agrees with the findings of Burgess et al. (2010), who report a yearly average accumulation of 0 to +0.18 m of water equivalent in the lower region of the Kangerlussuaq catchment area.

In the "wetter" upper ablation zone, at KAN_M and S9, the winter preceding the 2010 melt season indeed received a relatively small amount of snow accumulation: ~0.6 m, which is one third less than the year before. These are both low amounts of accumulation though, compared to other regions of the Greenland ice sheet such as the south or southeast where several metres of snow can accumulate in the ablation zone each year. Whereas the lower amount of wintertime accumulation in the upper ablation zone, and possibly at higher altitude (measurements lacking), will have had some influence on the high 2010 melt, it is third to the consequences of temperature and albedo mentioned above, given the relatively short time it takes for the snow to melt at the start of the melt season.

3.4 Surface melt and ablation

The measured time series of surface height change at the 6 weather stations is plotted in Fig. 5, along with the modelled values in the corresponding 100 m elevation bins. The time series start in September 2008, when the three-station K-transect (S5, S6, S9) was supplemented with KAN weather stations. Dashed coloured lines show model calculations that made use of the unaltered MODIS albedo product, while solid coloured lines represent model runs using calibrated MODIS albedo. The amount and time-evolution of ablation is modelled accurately judging from the agreement between the measurements and model results making use of calibrated MODIS albedo input, especially at low elevation (S5 and KAN_L). Uncalibrated MODIS input produces larger ablation than what was measured at all sites. Since both measured albedo at the weather stations and the overestimation of ablation without MODIS calibration suggest that the uncalibrated MODIS values are too low for this region, we will only focus on the calibrated MODIS results from hereon. Otherwise, our model output has not been calibrated in any way, with the exception of the precipitation parameterization.

A few minor mismatches exist between measured and modelled values, most notably at S6. A perfect agreement is not to be expected, since weather stations provide point measurements, while the model produces values for areas of tens to hundreds of square kilometres, with a mean elevation differing from those of the weather stations. Especially spatial albedo variability can be large and cause considerable differences in ablation over short distances – which is exactly why we use MODIS albedo in this study, and keep away from spatial interpolation of this variable.

Based on Fig. 5 we have confidence in the model performance and can look into the differences in net ablation between 2009 and 2010. In 2009, net ablation at low elevations was about 4 m of ice equivalent, which is a common value as documented by van den Broeke et al. (2008), who measured a mean yearly ablation of about 4.3 m ice eq. at S5 over the hydrological years 2004–2007, which were mostly warmer than 2009 (Fig. 2). Our ablation values for 2009 are slightly exceeding those for most years

TCD
5, 2319–2347, 2011

in a study by Mernild et al. (2010), who modelled meltwater run-off for the Kangerlussuaq catchment area for 1979–2008, largely based on the off-ice DMI meteorological time series in Kangerlussuaq. In our results, 2010 ablation (∼ 5 m at low elevation) exceeded all reported values from previous years. Figure 5 shows that relative differences between 2009 and 2010 are larger in the upper ablation zone (green and yellow lines).

An advantage of surface mass budget studies using energy balance modelling is that we can quantify the energy sources that contribute to ablation. Figure 6 shows the mean surface energy balance components per elevation bin for June, July and August. Predictably, energy available for melt decreased with elevation, both in 2009 (dashed black line) and 2010 (solid black line), averaging at over 150 $\mathrm{Wm^{-2}}$ in the lower ablation zone. This energy was mostly supplied by solar radiation absorbed at the surface (yellow lines), which typically decreases with elevation due to increasing albedo. Net longwave radiation is a heat sink over the entire domain, becoming more dominant in the energy budget with elevation, but never exceeding 60 $\mathrm{Wm^{-2}}$ in absolute numbers. The opposite is the case for the turbulent sensible heat exchange between atmosphere and ice sheet surface, decreasing from roughly a 40 $\mathrm{Wm^{-2}}$ contribution to near-zero mean values in the accumulation zone. Latent heat exchange was only a small contributor over the elevation domain in both summers in Fig. 6, peaking at around –20 $\mathrm{Wm^{-2}}$ in the upper ablation zone. The sub-surface heat flux was even smaller, with negative near-zero values at all elevations.

Large differences are visible between the mean energy budgets in the summer of 2009 and 2010 (Fig. 6). Energy available for melt was similar between both years in the very lower and upper regions of our domain, but in between the 2010 melt energy exceeded that of our reference year 2009, e.g. by over 70 $\mathrm{Wm^{-2}}$ in the upper ablation zone around 1200 m elevation. Melt in 2010 exceeded 2009 totals by a substantial 44 % in the summer months, averaged over the entire elevation domain. In the lower ablation zone (below the 1000 m elevation bin, i.e. 950 m), where ablation is large in all years, the excess melt was 19 %. But in the upper ablation zone (1000–1400 m

TCD
5, 2319–2347, 2011

elevation bins, i.e. 950–1450 m), where generally less than 2 m ice eq. is ablated each year, summer melt excess reached 166 % in the three summer months, not even taking into account melt in May and September.

In the lower ablation zone (below the 1000 m elevation bin) the larger 2010 melt was for 74 % caused by a less negative net longwave radiation budget, i.e. by larger emission from a warmer (or moister) atmosphere. The remainder of the energy was provided by the turbulent heat fluxes – also due to higher atmospheric temperatures, while net shortwave radiation actually contributed 2.5 $\mathrm{W\,m^{-2}}$ less on average. This implies that we can fully attribute the 2010 melt excess at low elevation to high temperatures.

In the upper ablation zone (1000–1400 m elevation bins) we find that the larger melt energy is mostly caused by larger amounts of absorbed solar radiation (55 %), but that still a significant share (49 %) originates from the energy fluxes sensitive to air temperature. The excess energy (4 %) was drained by the sub-surface heat flux, which was more negative in 2010 than in 2009. These results are in qualitative agreement to Tedesco et al. (2011), who also identified high temperatures and low albedo as the causes of the 2010 melt anomaly, facilitated by low wintertime accumulation. Tedesco et al. (2008) came to similar conclusions for 2007, which was also a year with relatively high melt on the Greenland ice sheet and identified as high-frequency melt year by van den Broeke et al. (2011). The latter confirmed the occurrence of the 2007 and 2010 melt anomalies in the upper ablation zone (S9), chiefly caused by the melt – albedo feedback. Van den Broeke et al. (2011) also stated that interannual melt variability in the lower ablation zone is driven by the variability in the turbulent flux of sensible heat, as is the case in our study.

The basin hypsometry dictates that the surface area decreases rapidly with decreasing elevation, mainly because the glacier surface is steeper near the margin, but also because the ice flow converges into outlet glaciers. For instance, the 500 m elevation bin has a surface area of 62 $\mathrm{km^2}$, while the 1000 m bin is sized 185 $\mathrm{km^2}$. Thus the 2010 melt, which was most extreme in the higher regions of the ablation zone, was of even larger significance than is apparent from Fig. 5, because of the increasing surface area with elevation. This also means that the area in which albedo was the dominant cause of the melt anomaly is much larger than the area in which this was valid for temperature.

3.5 Surface meltwater production

The surface meltwater run-off equals cumulative ablation reduced by the meltwater that refreezes in snow and firn. Integrating the daily run-off values as calculated per elevation bin over the Kangerlussuaq catchment area, provides the total surface meltwater run-off as plotted in Fig. 7 for 2009 and 2010 (black lines). Surface meltwater run-off started early in 2010 (late April), and was larger than in 2009 throughout almost the entire melt season. Whereas 2009 only had a single distinct melt peak between days of year 190 and 200 (mid-July), the 2010 record is a succession of large melt peaks over a four-month period. The amplitude of the largest melt peak in 2009 ($\sim 0.10\,km^3\,d^{-1}$), however, is not much smaller than in 2010 ($\sim 0.11\,km^3\,d^{-1}$) around day 210. We do not consider the melt peak on day 245 (2 September) of 2010 to be realistic, since albedo (especially at low elevation) was dubiously low, e.g. 0.17 at in the 500 m elevation bin, even though this day was the warmest day of the year over the catchment area (third warmest in Kangerlussuaq). We calculate the total surface meltwater run-off for the Kangerlussuaq catchment to be $2.67\,km^3$ for 2009, and $6.56\,km^3$ for 2010 (145 % larger).

The meltwater that runs off is transported to the ice sheet bed and internal drainage channels via a network of surface channels, melt lakes and moulins. There are no fair-sized surface melt streams near the ice margin due to low-elevation crevasse fields. We observed moulins form and re-activate annually in virtually the entire ablation zone, efficiently draining the surface water. After passage through and underneath the ice sheet, the meltwater collects in the proglacial melt river that runs past the town of Kangerlussuaq. The freshwater discharge as estimated from water level measurements of the proglacial river, at the bridge in Kangerlussuaq, is also shown in Fig. 7.

TCD
5, 2319–2347, 2011

We note the resemblance between the calculated meltwater run-off and measured freshwater discharge, in terms of absolute values and timing of peaks. The total discharge as estimated from calculations at the bridge is 2.45 km^3 for 2009 and 5.34 km^3 for 2010, respectively 8 and 19 % lower than the calculated meltwater run-off. Although the difference can easily be explained by the measurement and modelling uncertainty in both records, we should point out that the discharge measurements do not cover the entire melt season, and thus its yearly total will be a lower estimate. Also, the run-off values for the glacier do not consider the sinks and sources in the proglacial tundra, such as precipitation, evaporation, and interaction with groundwater. Although we expect these sinks and sources to be small compared to the meltwater run-off from the ice sheet, we cannot expect a full agreement between our two records in Fig. 7. On top of this, a mismatch between the two records could be caused by storage in supra- and sub-glacial melt lakes, including the ice-dammed lake as discussed by Russell et al. (2011).

Most importantly though, subglacial meltwater routing is likely to be determined by the ice sheet's bottom topography, as the many moulins transport the meltwater away from the surface not far from where it originated. In this study, and to our knowledge all similar studies on the Greenland ice sheet up to this point, the surface topography is used for catchment delineation given a lack of information about the bedrock topography. We hand-drew the basin borders by intersecting surface elevation contours perpendicularly starting at the pro-glacial watersheds, which we preferred over e.g. standard software tools that have proven to perform poorly over smooth surfaces with a low aspect ratio such as an ice sheet. As van de Wal and Russell (1994) already concluded, a large uncertainty in meltwater run-off estimates remains due to missing information on the exact extent of the drainage area. Our glacier surface catchment area (12 574 km^2) turned out to be larger that reported in previous studies, such as by Mernild et al. (2010) (6130 km^2) and Hasholt et al., 2011 (9743 km^2). Only a bedrock map (which is currently in production by GAP project partners) can tell which catchment is more accurate. However, given that our 2010 run-off total exceeds the estimated discharge value more than in 2009, and more meltwater originated from a higher elevation in 2010, this could be an indication that the actual (subglacial) drainage area includes less of the upper ablation and accumulation zone than assumed in this study.

Looking more closely at the run-off and discharge peaks, we point out the delay between the two. Although it is hard to tell because of the smeared-out freshwater discharge, regulated in a funnel-like fashion by the drainage system of the ice sheet, Fig. 7 shows that peaks between run-off and discharge show smaller temporal lags after the peak of the melt season than before. Also, especially in 2010 the discharge became more variable after the melt peak of the season, more closely following meltwater run-off. This is expected for an evolving sub-glacial drainage system, which continuously increases its capacity until meltwater availability decreases in August (typically). The meltwater conduits in the ice do not close fast enough to disallow efficient passage of meltwater during the remainder of the melt season. This is also concluded from sub-glacial water pressure measurements in the region, which produced high values before the peak of the melt season, and lower ones after (Harper et al., 2010). The link between meltwater production, basal pressure, and ice velocity has been subject of several studies in recent years for the Kangerlussuaq region (Bartholomew et al., 2010; Palmer et al., 2011; Sundal et al., 2011), but falls out of the scope of this paper.

4 Conclusions

In 2010, atmospheric temperatures were record-setting in large parts of Greenland. In Kangerlussuaq in Southwest Greenland, the yearly average temperature was 2.7 standard deviations above the 1974–2010 average. Also over the ice sheet temperatures exceeded the near-average year 2009 throughout the melt season, especially in the upper ablation zone and lower accumulation zone and during the record-warm month of August.

Because of the early onset of melt in 2010, and the somewhat lower amount of accumulation in the preceding winter, surface albedo values were below the 2000–2010

TCD
5, 2319–2347, 2011

average as determined from MODIS imagery. This in turn allowed for a larger solar radiation absorption, resulting in higher melt (melt-albedo feedback). As a consequence, energy available for surface melt was 44 % larger in 2010 than in 2009, averaged for all elevations. In the upper ablation zone the 2010 melt excess even reached 166 %, compared to 2009. Whereas the warmer atmosphere caused increased melt over the entire elevation domain, in the upper ablation zone the low albedo allowed for higher solar radiation absorption rates, roughly contributing half to the melt increase. Run-off for the entire Kangerlussuaq catchment area in 2010 was calculated to be 145 % larger than in the previous year. This value is almost as large as the melt excess for the upper ablation zone (166 %) due to the catchment hypsometry, dictating that area increases with elevation. During warm episodes in the future we can expect a melt response of at least the same magnitude. The more often heavy melt years will occur, the more snow and firn surfaces will make place for bare ice, and the larger the melt response will be.

The modelled meltwater run-off from the Kangerlussuaq catchment area agrees well with discharge measurements taken in the proglacial river system at the bridge in Kangerlussuaq. We found that modelled run-off was 8 and 19 % larger than the measured discharge in 2009 and 2010, respectively. The most plausible explanation of the difference is that the Kangerlussuaq catchment area in this study is larger than in reality. The exact size of the area is not known up to this point, since the bedrock topography, which determines the catchment delineation, is unknown for this region of the ice sheet. Efforts in the glaciological community are ongoing to produce a much-needed detailed bedrock map of the region, allowing us to more accurately determine the meltwater production in the Kangerlussuaq catchment area in future run-off studies.

Comparing meltwater production and freshwater discharge in more detail, we found that where 2009 had a single outstanding peak in its melt season, 2010 saw a large meltwater production throughout the entire summer. Following the peak in the melt season, meltwater was transported through the glacial hydrological drainage system more efficiently, visible as a reduction in the lag between calculated melt and measured discharge.

TCD
5, 2319–2347, 2011

Acknowledgements. Funding for this work was provided by the Greenland Analogue Project (GAP), a collaborative project funded by the nuclear waste management organizations in Sweden (Svensk Kärnbränslehantering AB), Finland (Posiva Oy) and Canada (NWMO). The surface melt component of GAP is run in collaboration with the Programme for Monitoring of the Greenland Ice Sheet (PROMICE). This is a PROMICE publication.

References

Bartholomew, I., Nienow, P., Mair, D., Hubbard, A., King, M. A., and Sole, A.: Seasonal evolution of subglacial drainage and acceleration in a Greenland outlet glacier, Nat. Geosci., 3, 408–411, 2010.

Box, J. E.: Survey of Greenland instrumental temperature records: 1873–2001, Int. J. Climatol., 22, 1829–1847, 2002.

Box, J. E., Ahlstrøm, A., Cappelen, J., Fettweis, X., Decker, D., Mote, T., van As, D., van de Wal, R. S. W., Vinther, B., and Wahr, J.: Greenland [in "State of the Climate in 2010"], B. Am. Meteorol. Soc., 92 (6), 161–171, 2011.

Brock, B. W., Willis, I. C., and Shaw, M. J.: Measurement and parameterization of aerodynamic roughness length variations at Haut Glacier d'Arolla, Switzerland, J. Glaciol., 52, 281–297, 2006.

Burgess, E. W., Forster, R. R., Box, J. E., Mosley-Thompson, E., Bromwich, D. H., Bales, R. C., and Smith, L. C.: A spatially calibrated model of annual accumulation rate on the Greenland Ice Sheet (1958–2007), J. Geophys. Res., 115, F02004, doi:10.1029/2009JF001293, 2010.

Csatho, B., Schenk, T., Van der Veen, C. J., and Krabill, W. B.: Intermittent thinning of Jakobshavn Isbrae, West Greenland, since the Little Ice Age, J. Glaciol., 54 (184), 131–144, 2008.

Harper, J. T., Humphrey, N. F., Johnson, J. V., Meierbachtol, T. W., Brinkerhoff, D. J., and Landowski, C. M.: Integrating borehole measurements with modeling of englacial and basal conditions, Western Greenland, Abstract C42A-03 presented at 2010 Fall Meeting, AGU, San Francisco, CA, USA, 13–17 December, 2010.

Hasholt, B., Mikkelsen, A. B., Larsen, M. A. D., and Holtegaard Nielsen, M.: Observations of runoff and sediment and dissolved loads from the Greenland ice sheet at Kangerlussuaq, West Greenland, 2007 to 2010, J. Glaciol., submitted, 2011.

Howat, I. M., Ahn, Y., Joughin, I., van den Broeke, M. R., Lenaerts, J. T. M., and Smith, B.:

Mass balance of Greenland's three largest outlet glaciers, 2000–2010, Geophys. Res. Lett., 38, L12501, doi:10.1029/2011GL047565, 2011.
Khan, S. A., Wahr, J., Bevis, M., Velicogna, I., and Kendrick, E.: Spread of ice mass loss into Northwest Greenland observed by GRACE and GPS, Geophys. Res. Lett., 37, L06501, doi:10.1029/2010GL042460, 2010.
Mernild, S. H., Liston, G. E., Steffen, K., van den Broeke, M., and Hasholt, B.: Runoff and mass-balance simulations from the Greenland Ice Sheet at Kangerlussuaq (Søndre Strømfjord) in a 30-year perspective, 1979–2008, The Cryosphere, 4, 231–242, doi:10.5194/tc-4-231-2010, 2010.
Palmer, S., Shepherd, A., Nienow, P., and Joughin, I.: Seasonal speedup of the Greenland Ice Sheet linked to routing of surface water, Earth Planet. Sc. Lett., 302, 423–428, 2011.
Pritchard, H. D., Arthern, R. J., Vaughan, D. G., and Edwards, L. A.: Extensive dynamic thinning on the margins of the Greenland and Antarctic ice sheets, Nature, 461 (7266), 971–975, 2009.
Rignot, E. and Kanagaratnam, P.: Changes in the velocity structure of the Greenland ice sheet, Science, 311, 986–990, 2006.
Russell, A. J., Carrivick, J. L., Ingeman-Nielsen, T., Yde, J. C., and Williams, M.: A new cycle of jökulhlaups at Russell Glacier, Kangerlussuaq, West Greenland, J. Glaciol., 57 (202), 238–246, 2011.
Schaaf, C. B., Wang, Z., and Strahler, A. H.: Commentary on Wang and Zender – MODIS snow albedo bias at high solar zenith angles relative to theory and to in situ observations in Greenland, Remote Sens. Environ., 115, 1296–1300, 2011.
Schrama, E., Wouters, B., and Vermeersen, B.: Present Day Regional Mass Loss of Greenland Observed with Satellite Gravimetry, Surv. Geophys., Springer Netherlands, doi:10.1007/s10712-011-9113-7, 2011.
Smeets, C. J. P. P. and van den Broeke, M. R.: Temporal and spatial variation of momentum roughness length in the ablation zone of the Greenland ice sheet, Bound.-Lay. Meteorol., 128, 315–338, 2008.
Sundal, A. V., Shepherd, A., Nienow, P., Hanna, E., Palmer, S., and Huybrechts, P.: Melt-induced speed-up of Greenland ice sheet offset by efficient subglacial drainage, Nature, 469, 521–524, doi:10.1038/nature09740, 2011.
Tedesco, M., Serreze, M., and Fettweis, X.: Diagnosing the extreme surface melt event over southwestern Greenland in 2007, The Cryosphere, 2, 159–166, doi:10.5194/tc-2-159-2008,

2008.
Tedesco, M., Fettweis, X., van den Broeke, M. R., van de Wal, R. S. W., Smeets, C. J. P. P., Van de Berg, W. J., Serreze, M. C., and Box, J. E.: The role of albedo and accumulation in the 2010 melting record in Greenland, Environ. Res. Lett., 6 pp, 014005, doi:10.1088/1748-9326/6/1/014005, 2011.
van As, D.: Warming, glacier melt and surface energy budget from weather station observations in the Melville Bay region of Northwest Greenland, J. Glaciol., 57(202), 208220, doi:10.3189/002214311796405898, 2011.
van As, D., Fausto, R. S., and the PROMICE project team: Programme for Monitoring of the Greenland Ice Sheet (PROMICE): first temperature and ablation records, Geol. Surv. Den. Greenl., 23, 73–76, 2011.
van den Broeke, M. R., van As, D., Reijmer, C. H., and van de Wal, R. S. W.: Assessing and improving the quality of unattended radiation observations in Antarctica, J. Atmos. Ocean. Tech., 21 (9), 1417–1431, 2004.
van den Broeke, M., Smeets, P., Ettema, J., van der Veen, C., van de Wal, R., and Oerlemans, J.: Partitioning of melt energy and meltwater fluxes in the ablation zone of the west Greenland ice sheet, The Cryosphere, 2, 179–189, doi:10.5194/tc-2-179-2008, 2008.
van den Broeke, M., Bamber, J., Ettema, J., Rignot, E., Schrama, E., Van de Berg, W. J., Van Meijgaard, E., Velicogna, I., and Wouters, B.: Partitioning recent Greenland mass loss, Science, 326, 984–986, 2009.
van den Broeke, M. R., Smeets, C. J. P. P., and van de Wal, R. S. W.: The seasonal cycle and interannual variability of surface energy balance and melt in the ablation zone of the west Greenland ice sheet, The Cryosphere, 5, 377–390, doi:10.5194/tc-5-377-2011, 2011.
van de Wal, R. S. W. and Russell, A. J.: A comparison of energy balance calculations, measured ablation and meltwater runoff near Søndre Strømfjord, West Greenland, Global Planet. Change, 9, 29–38, 1994.
Wang, X. and Zender, C. S.: MODIS snow albedo bias at high solar zenith angles relative to theory and to in situ observations in Greenland, Remote Sens. Environ., 114, 563–575, 2010.

Table 1. Metadata for the automatic weather stations on the Greenland ice sheet used in this study.

Station name	Latitude (° N)	Longitude (° W)	Elevation (m)	Date of placement
S5	67° 6′	50° 7′	460	1 Sep 2003
KAN_L	67° 6′	49° 56′	670	1 Sep 2008
S6	67° 5′	49° 23′	1020	1 Sep 2003
KAN_M	67° 4′	48° 49′	1280	2 Sep 2008
S9	67° 3′	48° 14′	1510	1 Sep 2003
KAN_U	67° 0′	47° 1′	1830	4 Apr 2009

TCD
5, 2319–2347, 2011

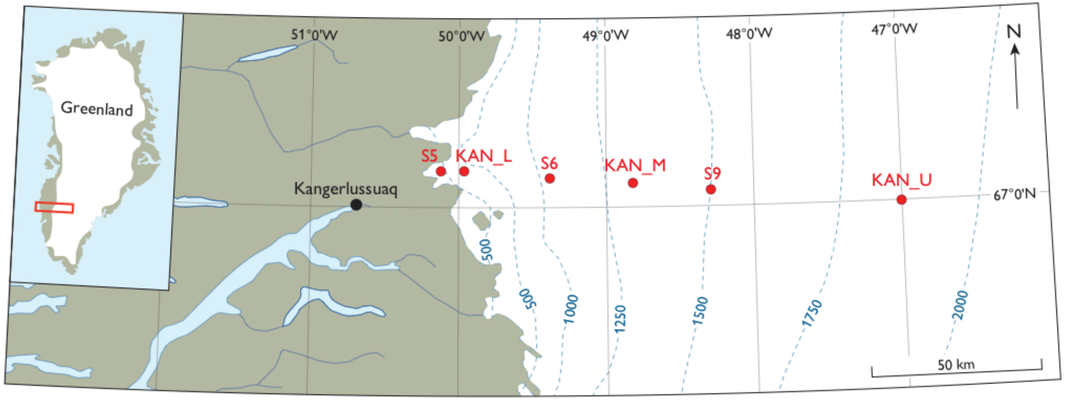

Fig. 1. Map of Southwest Greenland including the positions of the automatic weather stations used for this study.

TCD
5, 2319–2347, 2011

Greenland surface mass budget and melt in 2010

D. van As et al.

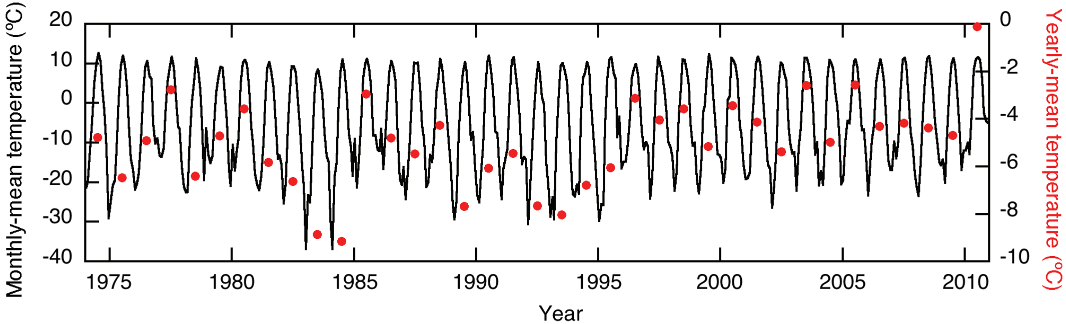

Fig. 2. Monthly-mean (black line) and yearly-mean (red dots) temperatures at the town of Kangerlussuaq.

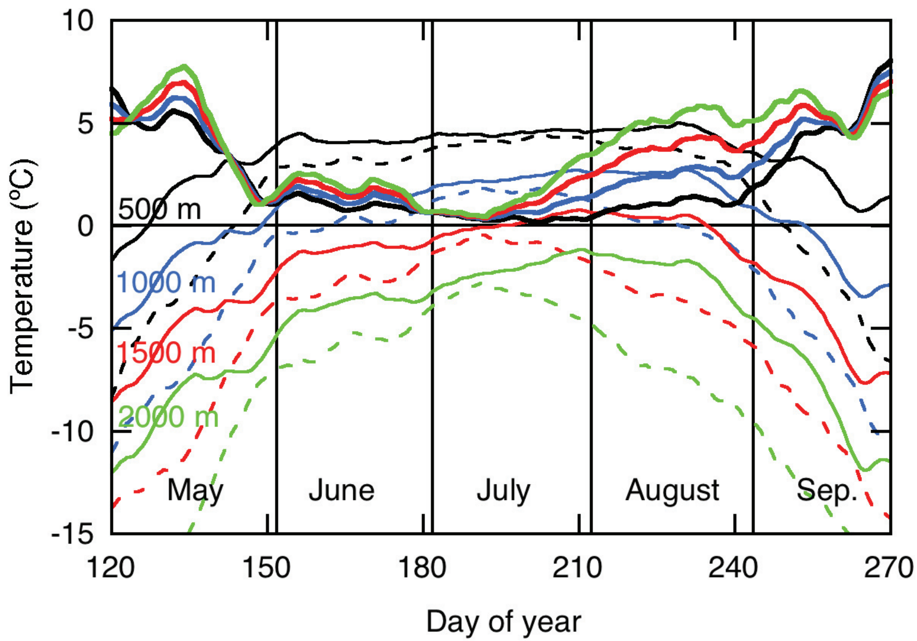

Fig. 3. Thirty-day running-mean near-surface temperature over the ice sheet at 500 m (black), 1000 m (blue), 1500 m (red) and 2000 m (green) elevation above sea level for 2009 (dashed lines) and 2010 (solid lines). Thick lines give the 2010–2009 difference with identical colour coding.

TCD
5, 2319–2347, 2011

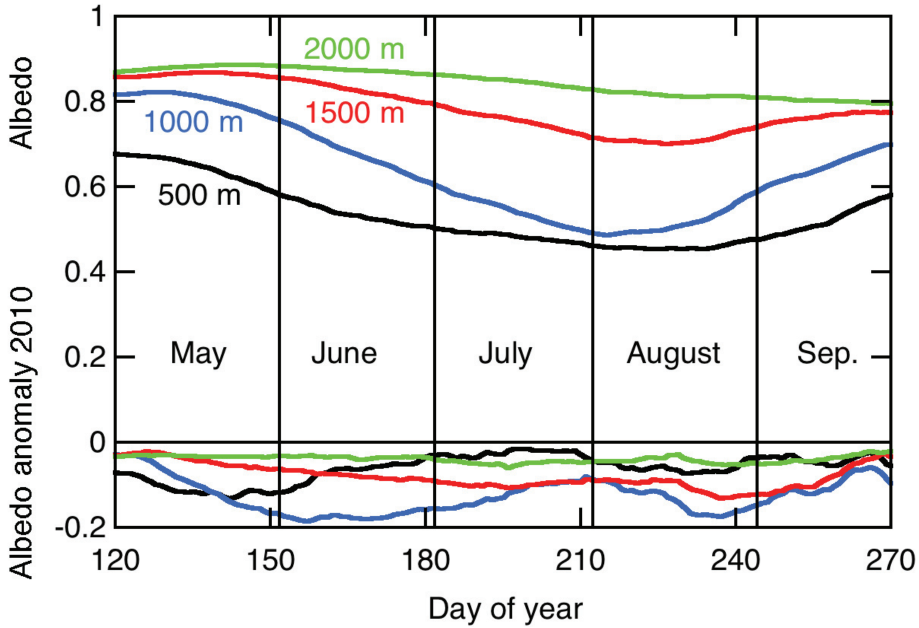

Fig. 4. Thirty-day running mean (calibrated) albedo at 500 m (black), 1000 m (blue), 1500 m (red) and 2000 m (green) elevation above sea level for the MODIS period (2000–2010). The lower lines give the 2010 albedo anomaly with identical colour coding.

TCD
5, 2319–2347, 2011

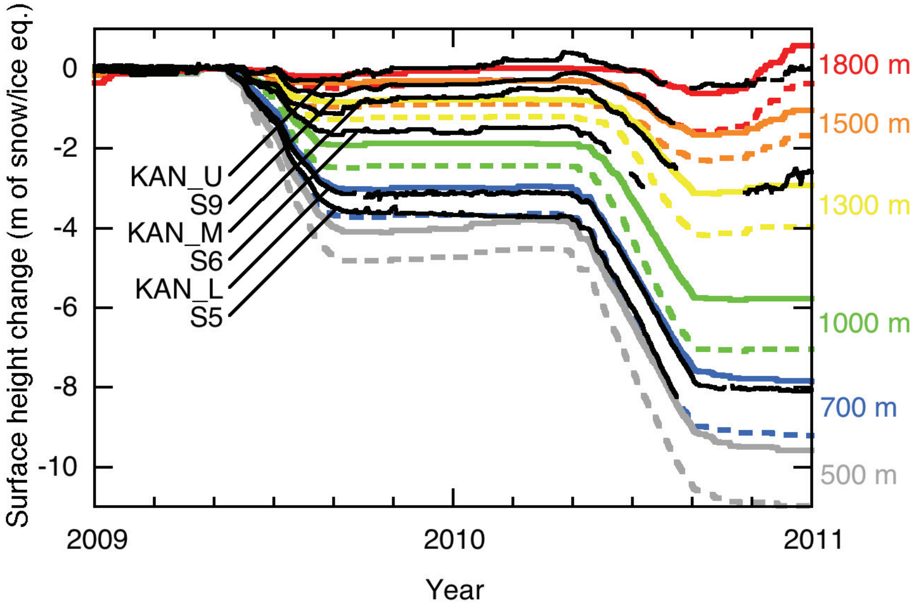

Fig. 5. Measured surface height change due to accumulation and ablation at the weather stations (black), and modelled values within the corresponding elevation bin (colours), with (solid) and without (dashed) MODIS albedo correction. N.B.: for late 2010 measured and modelled data series have been aligned after data gaps.

TCD
5, 2319–2347, 2011

Greenland surface mass budget and melt in 2010

D. van As et al.

Title Page
Abstract Introduction
Conclusions References
Tables Figures
◄ ►
Back Close
Full Screen / Esc
Printer-friendly Version
Interactive Discussion

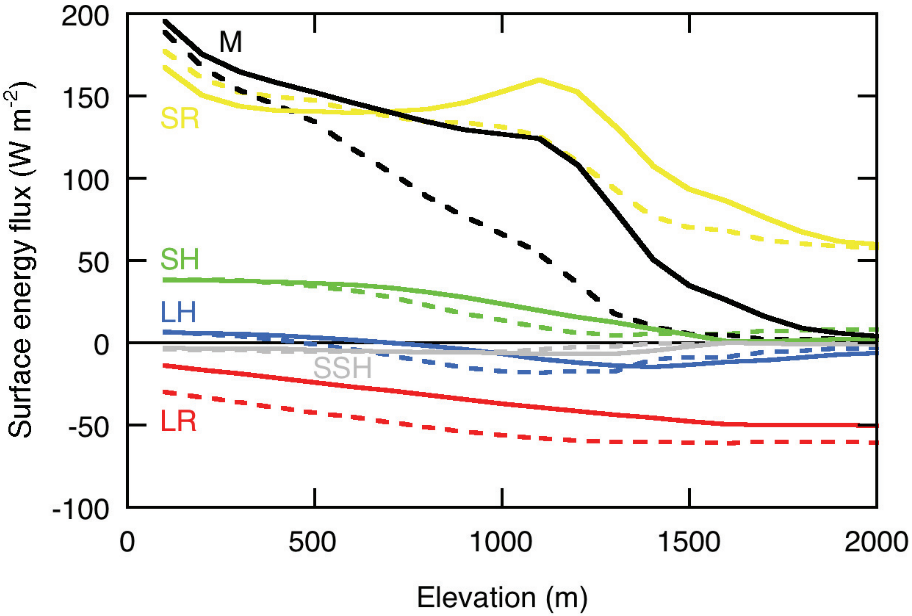

Fig. 6. Mean surface energy budget components for June, July and August in 2009 (dashed lines) and 2010 (solid lines) versus elevation. Net shortwave radiation: yellow, net longwave radiation: red, sensible heat flux: green, latent heat flux: blue, sub-surface heat flux: grey, and energy available for melt: black.

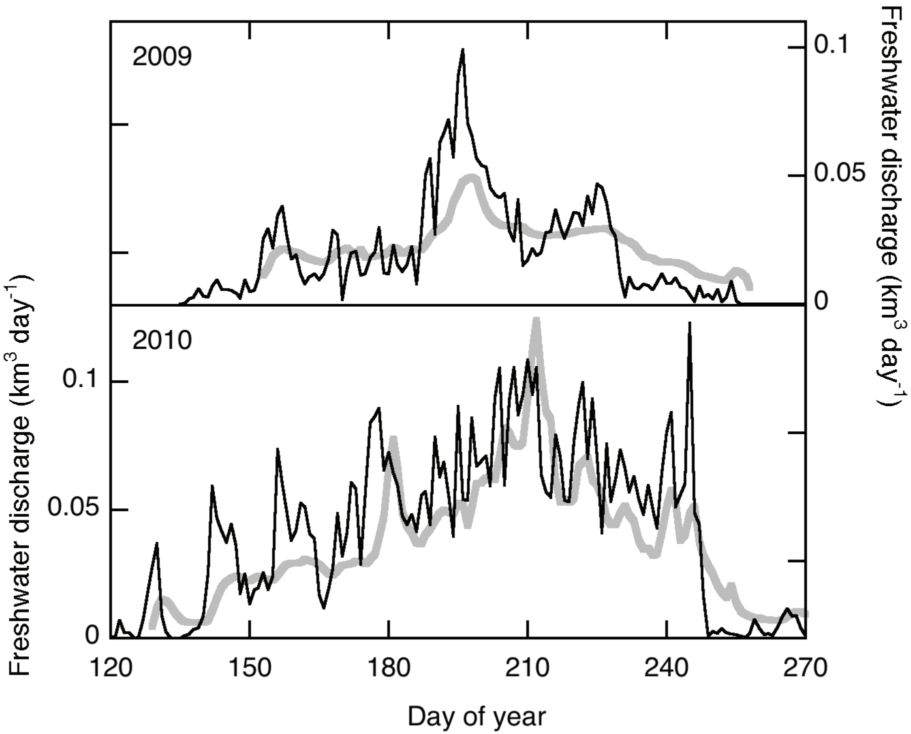

Fig. 7. Calculated daily totals of surface meltwater run-off for the Kangerlussuaq catchment area (black) and the freshwater flux estimated from river depth measurements (grey) for 2009 and 2010.

TCD
5, 2319–2347, 2011